Chemical shift assignments and folding topology of the Ras-binding domain of human Raf-1 as determined by heteronuclear three-dimensional NMR spectroscopy.

ARTICLE *in* BIOCHEMISTRY · JUNE 1994

Impact Factor: 3.02 · Source: PubMed

6 AUTHORS, INCLUDING:

David Waugh
National Cancer Institute (USA)
137 PUBLICATIONS **5,895** CITATIONS
SEE PROFILE

Julie E Scheffler
Johnson & Johnson
28 PUBLICATIONS **897** CITATIONS
SEE PROFILE

Biochemistry

 Volume 33, Number 25 June 28, 1994

Accelerated Publications

Chemical Shift Assignments and Folding Topology of the RAS-Binding Domain of Human RAF-1 As Determined by Heteronuclear Three-Dimensional NMR Spectroscopy

S. Donald Emerson, David S. Waugh, Julie E. Scheffler, Kwei-Lan Tsao, Kathleen M. Prinzo, and David C. Fry*

Roche Research Center, Hoffmann-La Roche, Inc., Nutley, New Jersey 07110

Received March 3, 1994; Revised Manuscript Received May 6, 1994®

ABSTRACT: Raf-1 is a 74-kDa serine–threonine kinase which serves as the immediate downstream target of Ras in the cell growth signal transduction pathway. Recent genetic and biochemical experiments have demonstrated that (1) Ras interacts directly with the amino-terminal domain of Raf and (2) residues 51–131 of the Raf sequence are sufficient to mediate this interaction [Vojtek, A. B., Hollenberg, S. M., & Cooper, J. A. (1993) *Cell 74*, 205–214]. We have expressed a corresponding segment of the human Raf sequence (Raf_{55-132}) in *Escherichia coli* as a fusion with maltose binding protein. The fusion protein was purified by affinity chromatography and cleaved at a pre-engineered site with factor Xa protease to liberate the 78-residue fragment of Raf. Raf_{55-132} bound to Ras with high affinity in a competition assay with GAP. An unlabeled version of Raf_{55-132} was studied by 2D homonuclear NMR, and uniformly ^{15}N- and $^{13}C/^{15}N$-labeled versions of Raf_{55-132} were studied by 2D and 3D heteronuclear NMR. Nearly complete sequence-specific assignments were made for the backbone H^N, H^α, ^{15}N, and $^{13}C^\alpha$ resonances. NOEs were used to determine regions of secondary structure and the overall folding topology. Raf_{55-132} is an independently folded domain composed of a five-stranded β-sheet, a three-turn α-helix, and possibly an additional one-turn helix. Its structure resembles that of ubiquitin, even though there is no more than 11% sequence homology between the two proteins.

The proto-oncoprotein c-Raf-1 is an essential participant in the cell growth signal transduction pathway (Heidecker et al., 1992). Substantial evidence indicates that Raf-1 is the immediate downstream target of the protein Ras[1] (Moodie et al., 1993; Vojtek et al., 1993; Van Aelst et al., 1993; Warne et al., 1993; Williams et al., 1993; Zhang et al., 1993). Raf-1 is a serine–threonine protein kinase, and Ras apparently has a role in regulating this activity. It has recently been demonstrated that Raf-1 interacts directly with the GTP-bound form of Ras both *in vitro* and *in vivo* (Moodie et al., 1993; Vojtek et al., 1993; Van Aelst et al., 1993; Warne et al., 1993; Zhang et al., 1993).

Many human cancers are associated with mutant forms of Ras that tend to remain in the GTP-bound state, resulting in continuous signal transmission (Barbacid, 1987). A molecule that blocks the Ras–Raf interaction would interrupt this signal and might have therapeutic value. Toward the design of such

® Abstract published in *Advance ACS Abstracts*, June 1, 1994.

[1] Abbreviations: Raf_{55-132}, a polypeptide consisting of residues 55–132 of human c-Raf-1 with an additional alanine residue at the N-terminus; Ras, the 21-kDa protein product of the *ras* oncogene; GAP, GTPase activating protein; NMR, nuclear magnetic resonance; EDTA, ethylenediaminetetraacetic acid; PMSF, phenylmethanesulfonylfluoride; IPTG, isopropyl β-D-thiogalactopyranoside; DTT, dithiothreitol; IC_{50}, concentration which results in 50% inhibition; NOE, nuclear Overhauser effect; NOESY nuclear Overhauser effect spectroscopy; COSY, correlation spectroscopy; TOSCY, total correlation spectroscopy; HNCA, amide proton to nitrogen to α-carbon intraresidue correlation; HN(CO)CA, amide proton to nitrogen to α-carbon interresidue correlation via carbonyl; HSQC heteronuclear single-quantum correlation; HMQC, heteronuclear multiple-quantum correlation; INEPT, insensitive nucleus enhancement by polarization transfer; 1D, one dimensional; 2D, two dimensional; 3D, three dimensional.

0006-2960/94/0433-7745$04.50/0

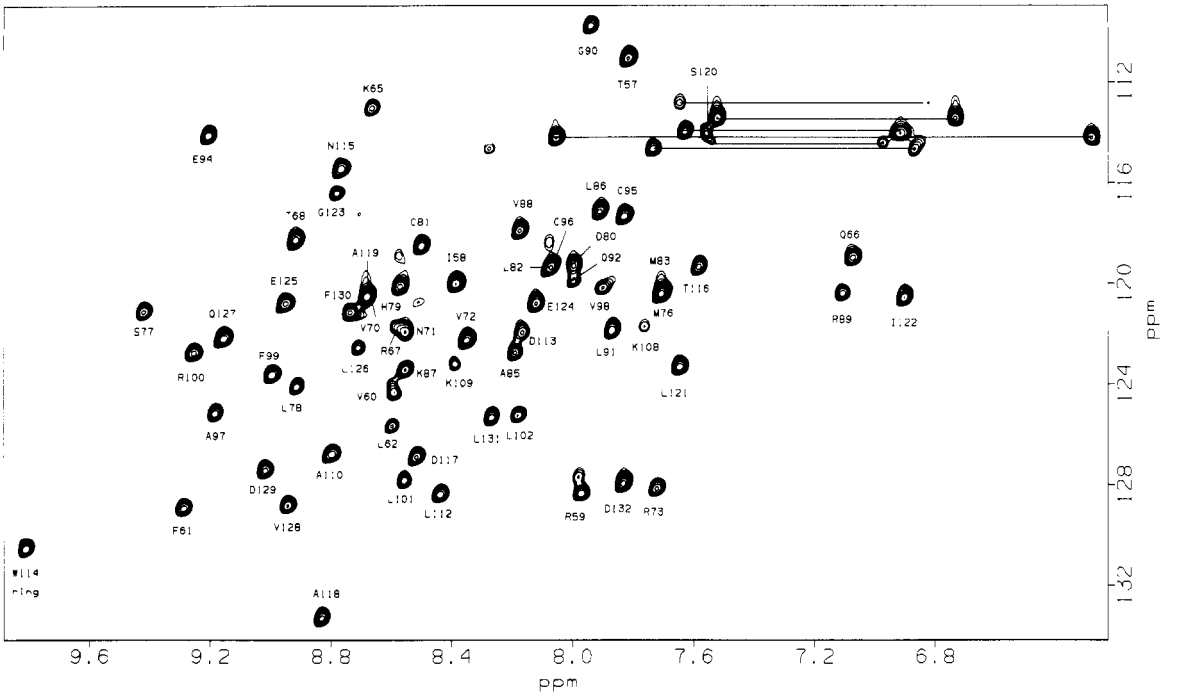

FIGURE 1: 2D ^{1}H–^{15}N HSQC spectrum of Raf_{55-132}. The sample consisted of 1.7 mM uniformly $^{13}C/^{15}N$-labeled Raf_{55-132}, 10 mM sodium acetate-d_3, pH 7.3, 0.1 mM DTT, and 90% H_2O/10% D_2O, at 25 °C. Correlations between backbone H^N and ^{15}N resonances are labeled. The correlation between the tryptophan ring $H^{N\epsilon}$ and $^{15}N\epsilon$ is also shown. Cross peaks involving asparagine and glutamine side-chain NH_2 resonances are connected by horizontal lines.

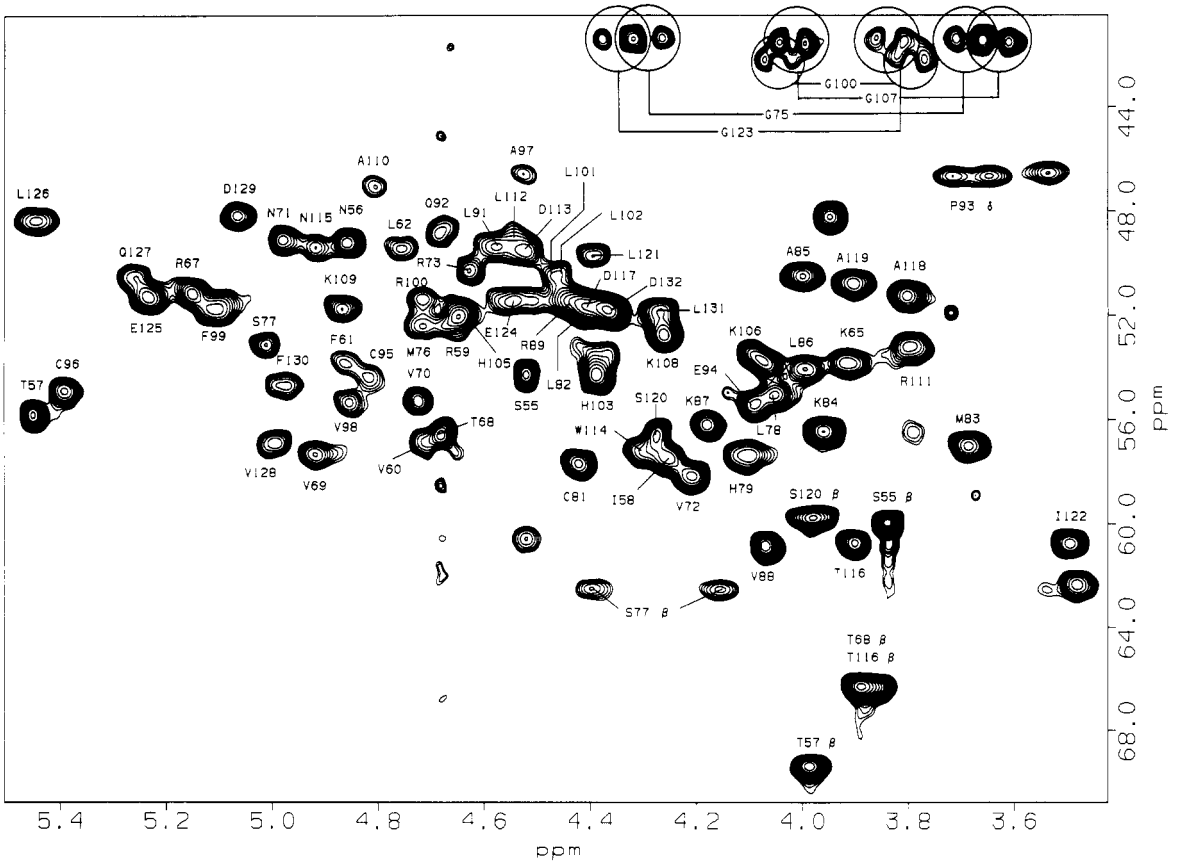

FIGURE 2: 2D ^{1}H–^{13}C HMQC spectrum of Raf_{55-132}. The sample consisted of 1.5 mM uniformly $^{13}C/^{15}N$-labeled Raf_{55-132}, 9 mM sodium acetate-d_3, pH 7.3, 0.1 mM DTT, and 100% D_2O, at 25 °C. Correlations between backbone H^α and $^{13}C^\alpha$ resonances are labeled. Correlations between serine and threonine H^β and $^{13}C^\beta$ resonances are also shown.

a molecule, we are studying the structural details of the Ras–Raf interaction.

Raf-1 is a 74-kDa protein which contains, in addition to a C-terminal catalytic domain (CR-3), two other highly conserved regions termed CR–1 and CR–2 (Heidecker et al., 1992). The Ras-binding region is located within CR–1, which encompasses residues 62–194 (Morrison, 1990). Recently, Vojtek et al. (1993) employed a variation of the two-hybrid

screening procedure to identify fragments of CR-1 that are capable of binding with high affinity to Ras-GTP *in vivo*. Each of the active fragments included residues 51–131 of the Raf-1 sequence, suggesting that some or all of these residues are required for binding to Ras. This hypothesis was confirmed by expressing residues 55–132 of human Raf-1 as a C-terminal extension of the *Escherichia coli* maltose binding protein and demonstrating that this 78-residue fragment of Raf, either by itself or in the context of the fusion protein, is capable of binding to Ras with high affinity *in vitro* (Scheffler et al., 1994).

Here we report the results obtained from multidimensional NMR experiments performed on the Ras-binding domain of Raf-1 (Raf_{55-132}). Raf_{55-132} was found to be a highly structured protein, with a completely self-contained folding topology. ^{15}N- and $^{13}C/^{15}N$-labeled versions of the protein were produced and used to acquire a full set of 2D and 3D homonuclear and heteronuclear NMR data. Analysis of these data led to a nearly complete assignment of the backbone H^N, H^α, ^{15}N, and $^{13}C^\alpha$ resonances of the protein, along with many side-chain resonances. NOEs were used to determine the locations of secondary structural elements and the overall topology.

MATERIALS AND METHODS

Sample Preparation. Expression and purification of Raf_{55-132} have been described in detail (Scheffler et al., 1994). In short, pDW333, a plasmid vector that expresses residues 55–132 of human c-Raf-1 (Bonner et al., 1986) as a C-terminal extension of the *E. coli* maltose binding protein, was established in *E. coli* CT14 cells by a standard method (Chung et al., 1989). CT14 is a derivative of *E. coli* BL21/DE3 (Studier et al., 1991) with a defective *malE* gene (*malE50*::Tn10) and therefore produces no endogenous maltose binding protein. Transformed cells were grown in shake flasks at 37 °C. For uniform enrichment with ^{15}N, the cells were propagated in M9 medium (Sambrook et al., 1989) containing $^{15}NH_4Cl$ (Cambridge Isotopes), 0.2% D-glucose, 100 mg/mL ampicillin, and 20% (v/v) Celtone-N liquid (Martek). The same medium was used to achieve uniform enrichment with $^{13}C/^{15}N$, except that 0.1% of (U-$^{13}C_6$)-D-glucose (Cambridge Isotopes) was used instead of ^{12}C-D-glucose, and Celtone-CN (Martek) was used instead of Celtone-N. When the cells reached an A_{600} of approximately 0.8, IPTG was added to a final concentration of 0.4 mM. Three hours later, the cells were recovered by centrifugation and then frozen at −80 °C. Between 2 and 3 g of cells were obtained from each liter of medium.

The protein was purified by affinity chromatography on amylose resin (New England Biolabs) and cleaved with factor Xa (Pierce Chemical Co.) as described (Scheffler et al., 1994). The cleavage site was constructed such that the purified Raf_{55-132} protein contains an extra alanine, which is not part of the native Raf sequence, as its N-terminal residue. Separation of Raf_{55-132} from maltose binding protein was accomplished by adsorption to SP-Sepharose resin (Pharmacia). The high isoelectric point of Raf_{55-132} (pI = 8.8) ensured binding at pH 7.0, where factor Xa and maltose binding protein did not bind.

All NMR samples contained 0.1 mM DTT and 0.04% sodium azide. Aqueous (H_2O) samples contained 10% D_2O; 100% D_2O samples were prepared either by lyophilization and dissolution into D_2O ("100%" Cambridge Isotopes) or by ultrafiltration with D_2O-containing buffer. The volumes of samples were 630 or 375 μL for 5- or 4-mm Wilmad NMR tubes, respectively. Natural abundance NMR samples consisted of 0.7–1.0 mM Raf_{55-132}, in one of two buffer systems: 10 mM sodium acetate-d_3, 1.4 mM sodium phosphate, pH 5.3, or 10 mM sodium phosphate, pH 7.3. Samples uniformly enriched in ^{15}N and ^{13}C were as follows: aqueous 1.7 mM $^{13}C/^{15}N$ Raf_{55-132} and 10 mM sodium acetate-d_3, pH 7.3; and a D_2O solution of 1.5 mM $^{13}C/^{15}N$ Raf_{55-132} and 9 mM sodium acetate-d_3, pH 7.3. The sample enriched in ^{15}N contained 1.0 mM ^{15}N Raf_{55-132} and 25 mM sodium acetate-d_3, in aqueous solvent at pH 5.3.

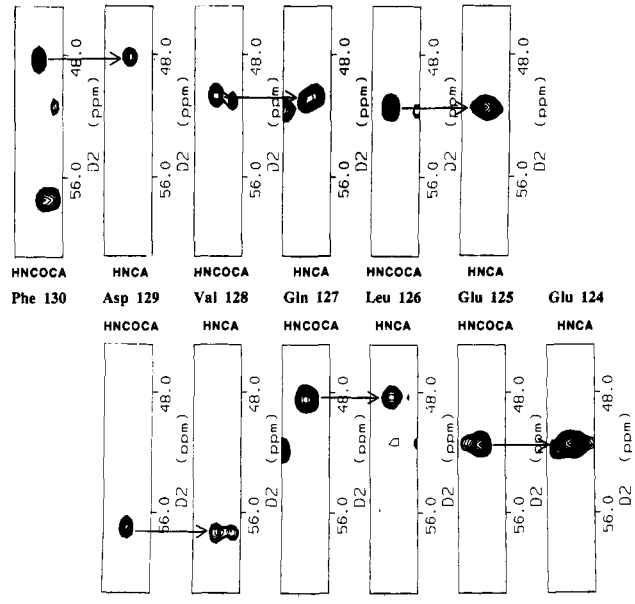

FIGURE 3: Strips of data from the 3D HN(CO)CA and HNCA spectra of Raf_{55-132} aligned to demonstrate the sequential assignment process. Each strip is a portion of the ^1H–$^{13}C^\alpha$ plane corresponding to a particular ^{15}N frequency. The bottom axis encompasses the H^N proton chemical shift of the indicated residue. Cross peaks in the HNCA spectra represent intraresidue H^N_i–$^{13}C^\alpha_i$ correlations. Arrows leading from HN(CO)CA spectra indicate sequential H^N_{i+1}–$^{13}C^\alpha_i$ connectivities. The sample consisted of 1.7 mM uniformly $^{13}C/^{15}N$-labeled Raf_{55-132}, 10 mM sodium acetate-d_3, pH 7.3, 0.1 mM DTT, and 90% H_2O/10% D_2O, at 25 °C.

Activity Assay. The Ras-binding activity of Raf_{55-132} was measured in a competition assay (Scheffler et al., 1994). A standard assay (Gibbs et al., 1988; Rubinfeld et al., 1991) was set up in which the GAP protein was added to Ras and allowed to accelerate its GTPase activity, as measured by release of γ-^{32}P from Ras-[γ-^{32}P]GTP, which was retained on a nitrocellulose filter. The ability of Raf_{55-132} to inhibit this interaction was measured and expressed as an IC_{50} value.

NMR Spectroscopy. NMR experiments were run on Varian UNITY-500 and UNITY*plus*-600 spectrometers. The sample temperature was 25 °C. Data were processed using FTNMR (Hare Research, Inc.) and FELIX (BioSym) software on VAX and Silicon Graphics computers. 2D TOCSY (Bruschweiler & Ernst, 1983) spectra of natural abundance Raf_{55-132} were acquired using both aqueous and D_2O solutions. TOCSY spin locks were executed for 45, 65, and 85 ms using the "clean" MLEV-17 (Griesinger et al., 1988) mixing scheme. 2D NOESY (Macura & Ernst, 1980) spectra were collected in H_2O using a NOE mixing time of 150 ms, and in D_2O using a 70-ms mixing time. A 2D DQF-COSY (Piantini et al., 1982) spectrum was collected using the unenriched sample in D_2O. A 2D ^1H–^{15}N HSQC (Bodenhausen & Ruben, 1980) spectrum was acquired using $^{13}C/^{15}N$ enriched Raf_{55-132} in H_2O, pH 7.3. Water suppression and selection of the heteronuclear coherence pathway were accomplished using a phase-sensitve pulsed field gradient approach (Davis et al., 1992). A gradient field strength of 30 Gauss/cm was used. A 9.9-ms gradient pulse was applied

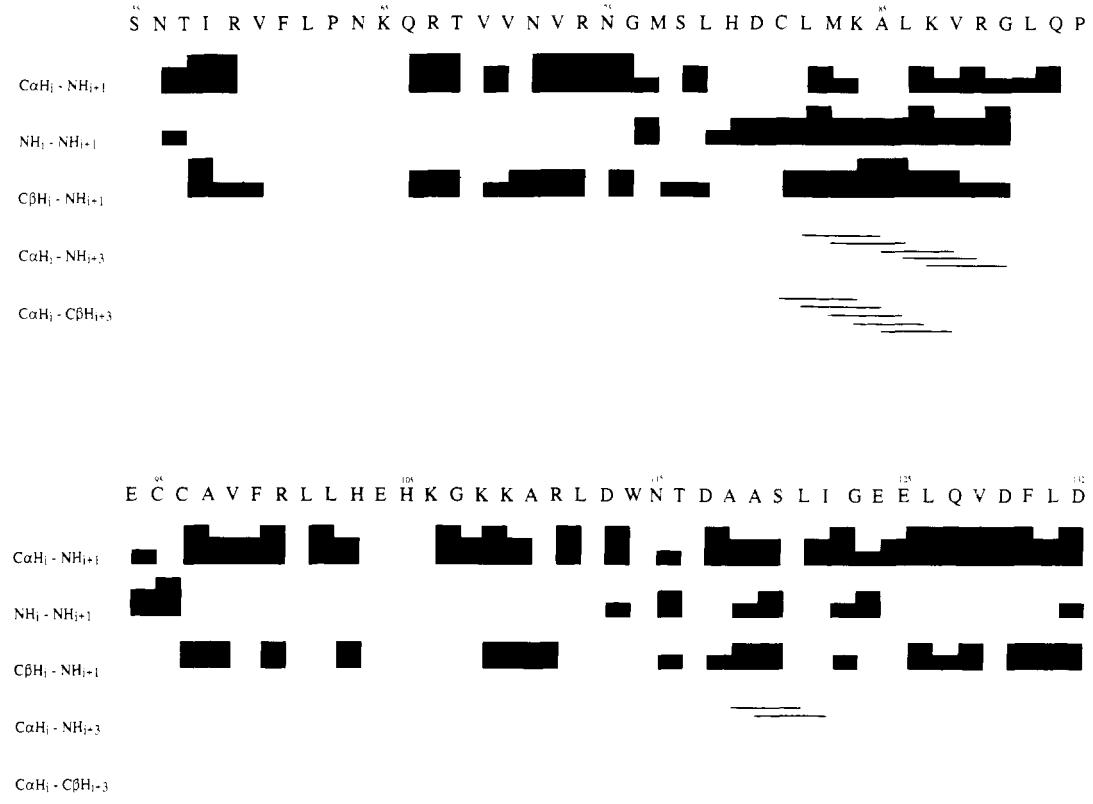

FIGURE 4: Graphic depiction of the commonly expected (i)–$(i + 1)$ and (i)–$(i + 3)$ NOEs which were observed for Raf_{55-132}. The height of each block corresponds to the magnitude of the NOE: small, medium, or large. The sample consisted of 1.0 mM Raf_{55-132}, 10 mM sodium acetate-d_3, 1.4 mM sodium phosphate, pH 5.3, 0.1 mM DTT, and 90% H_2O/10% D_2O, at 25 °C.

during the ^{15}N evolution time, and a 1.0-ms gradient pulse was applied during refocusing of ^1H magnetization in the reversed INEPT. The 1.0-ms gradient was flipped in order to select for P or N mode data. The P and N data were collected as separate hypercomplex pairs and combined to produce the phase-sensitive spectrum (Nagayama, 1986). The 3D ^1H–^1H–^{15}N NOESY-HSQC spectrum was acquired using ^{15}N-enriched Raf_{55-132} in H_2O solution, pH 5.3. Water suppression and heteronuclear coherence selection for F_2F_3 2D planes were accomplished with the same phase-sensitive pulsed field gradient approach described for the ^1H–^{15}N HSQC spectrum. Pure phase F_1F_3 planes were collected using the hypercomplex strategy with F_1-axial displacement (Marion et al., 1989). This spectrum was acquired with soft preirradiation ($\gamma H_2 = 20$ Hz) for 1.2 s in order to suppress exchange peaks from H_2O to H^N which obscure NOEs to H^αs that resonate at the water frequency. A 2D ^1H–^{13}C HMQC (Mueller, 1979) spectrum was acquired using $^{13}C/^{15}N$-enriched Raf_{55-132} in D_2O solution, pH 7.3. This same sample was used for the 2D ^1H–^{13}C HCCH-TOCSY (Bax et al., 1990) spectrum, which was acquired using DIPSI-3 (Shaka et al., 1988) spin locks of 18.3 and 45.7 ms. The 3D HNCA (Farmer et al., 1992) and HN(CO)CA (Kay et al., 1990) spectra were acquired using $^{13}C/^{15}N$-enriched Raf_{55-132} in H_2O solution, pH 7.3. The ^{13}C transmitter was placed in the center of the ^{13}CO region to facilitate selective decoupling of ^{13}CO carbons with the SEDUCE-1 scheme (McCoy & Mueller, 1992). The $^{13}C^\alpha$ pulses were given as shifted pulses at 54.7 ppm without changing the transmitter frequency (Patt, 1992).

RESULTS AND DISCUSSION

Characterization of Raf_{55-132}. Although Raf_{55-132} is only a fragment of a protein, initial 1D ^1H spectra revealed a wide diversity of chemical shifts, indicative of a well-ordered structure. Raf_{55-132} bound tightly to Ras in the GAP competition assay, exhibiting IC_{50} values of 90–100 nM. This level of activity was comparable to, or higher than, values reported for the full N-terminal domain of Raf (Raf_{1-257}) (Warne et al., 1993; Zhang et al., 1993). All samples were assayed following NMR data acquisition and found to retain full activity. However, lyophilization of the sample, or storage over long periods of time, was found to initiate a degradation of spectral quality due to the appearance of a minor, slightly shifted species for some resonances.

Assignment of Resonances. A full sequential assignment was accomplished in several steps. Initially, H^N–H^α–H^β connectivities were sought by analyzing the 2D TOCSY spectrum of the sample in H_2O at pH 5.3. These connectivity patterns could be clearly identified for 54 of the 78 residues in the protein. Patterns for the other residues were ambiguous due to overlap or incomplete due to unobservable exchange-broadened H^N resonances and unobservable H^α resonances saturated during preirradiation of the water signal. Additional connectivities were obtained by analyzing TOCSY and DQF-COSY spectra at pH 7.3 in both H_2O and D_2O, where chemical shift differences allowed problems of overlap to be resolved, and where several H^α resonances near the chemical shift of water could be observed. At this stage of the analysis, H^N–H^α–H^β connectivities were established for all but four of the non-proline residues.

Each identified H^N shift was then correlated to a ^{15}N chemical shift in the ^1H–^{15}N HSQC spectrum (Figure 1). Identification of the intraresidue backbone shifts was completed by correlating each ^1H–^{15}N pair to a $^{13}C^\alpha$ resonance in the 3D HNCA spectrum. These intraresidue sets were confirmed and extended by correlation of $^{13}C^\alpha$ to H^α resonances in the 2D ^1H–^{13}C HMQC spectrum (Figure 2) and correlation

Table 1: Chemical Shift Assignments for Raf_{55-132}[a]

	H^N						
	pH 7.3	pH 5.3	^{15}N	H^α	$^{13}C^\alpha$	H^β	other
S55				4.52	54.3	3.84	
N56		(8.76)	(123.8)	4.87	49.1	3.00, 2.84	
T57	7.82	(7.84)	111.0	5.46	56.0	3.98	$C\gamma H_3$ 1.02
I58	8.39	(8.40)	120.0	4.24	57.8	1.26	
R59	7.97	(7.97)	128.3	4.66	52.4	1.80	
V60	8.60	(8.59)	124.3	4.73	56.9	1.67	$C\gamma H_3$ 0.69
F61	9.30	(9.31)	128.9	4.88	54.1	3.23, 2.95	$C\delta H$ 7.27
L62	8.59	(8.59)	125.7	4.75	49.4	1.52	
P63							
N64					49.7		
K65	8.69	(8.68)	113.0	3.91	53.9	2.14, 2.04	
Q66	7.07	(7.07)	119.0	4.53	51.6	2.05, 1.90	
R67	8.61	(8.60)	121.9	5.14	51.4	1.73, 1.50	
T68	8.91	(8.93)	118.3	4.67	56.9	3.89	$C\gamma H_3$ 0.85
V69	8.11	(8.11)	(125.4)	4.91	57.4	1.86	$C\gamma H_3$ 0.85
V70	8.69	(8.68)	120.5	4.72	55.4	2.14	$C\gamma H_3$ 0.85, 0.70
N71	8.57	(8.55)	121.9	4.97	49.3	2.63	
V72	8.36	(8.33)	122.2	4.20	58.6	1.66	$C\gamma H_3$ 0.73, 0.66
R73	7.74	(7.67)	128.1	4.63	50.4	1.89, 1.69	
N74	8.59	(8.61)	(122.4)	4.37		2.75, 2.68	
G75	9.09	(9.13)	115.6	4.28, 3.69	41.7		
M76	7.70	(7.70)	120.4	4.72	52.6	2.30	
S77	9.40	(9.29)	121.1	4.99	53.3	4.39, 4.17	
L78	8.93	(9.01)	124.1	4.05	55.2	1.84, 1.69	
H79	8.58	(8.71)	120.1	4.10	57.8	3.27, 3.08	
D80	7.99	(8.04)	119.3		53.8	2.99	
C81	8.53	(8.67)	118.5	4.42	58.0	3.00, 2.86	
L82	8.07	(8.00)	119.4	4.40	51.9	1.96, 1.66	
M83	7.66	(7.44)	120.2	3.68	57.0	2.08, 1.89	
K84	8.51	(8.51)	(121.2)	3.97	56.5	1.82	
A85	8.23	(8.28)	122.7	3.98	50.7	1.32	
L86	7.90	(7.86)	117.2	3.98	54.4	1.67	
K87	8.56	(8.55)	123.4	4.17	56.4	1.97, 1.91	
V88	8.17	(8.13)	117.9	4.06	61.3	2.26	$C\gamma H_3$ 1.07, 1.04
R89	7.11	(7.13)	120.4	4.42	51.6	1.74, 1.56	
G90	7.94	(7.95)	109.8	4.04, 3.80	42.0		
L91	7.88	(7.87)	121.9	4.61	49.5	1.55, 1.50	
Q92	7.98	(7.92)	119.9	4.70	48.9	1.97	
P93					62.5		$C\delta H_2$ 3.71, 3.64
E94	9.17	(9.08)	114.1	4.08	55.7		
C95	7.82	(7.77)	117.4	4.82	54.4	3.44, 3.16	
C96	8.06	(8.05)	119.4	5.39	55.0	2.98	
A97	9.20	(9.24)	125.2	4.53	46.6	1.13	
V98	7.93	(7.99)	120.2	4.88	55.6	1.04	$C\gamma H_3$ 0.19, –0.20
F99	8.99	(8.96)	123.6	5.10	51.9	2.67, 2.55	$C\delta H$ 6.88; $C\epsilon H$ 7.23
R100	9.29	(9.30)	122.8	4.72	51.6	1.84	
L101	8.57	(8.60)	127.8	4.43	51.4		
L102	8.17	(8.13)	125.2	4.44	50.6	1.65, 1.51	
H103		(8.73)	(122.4)	4.38	54.4	3.06	
E104		(8.80)	(119.7)	4.07		2.05	
H105	7.66	(7.76)	(118.7)	4.62	51.5	3.09, 2.86	
K106		(8.36)	(122.5)	4.10	53.3	1.77	
G107	8.47	(8.46)	(112.0)	4.03, 3.63	41.5		
K108	7.80	(7.90)	121.7	4.28	53.1	1.77	
K109	8.40	(8.43)	123.2	4.88	51.9	1.53	
A110	8.80	(8.79)	126.8	4.80	46.9	1.36	
R111		(8.89)	(127.6)	3.80	53.2	1.68	
L112	8.44	(8.42)	128.4	4.54	48.8		
D113	8.16	(8.16)	121.9	4.54	49.5	2.67, 2.52	
W114		(8.93)	(128.3)	4.31	57.4	3.38, 3.14	C2H 7.46; C4H 7.46; C5H 6.80; C6H 6.67; C7H 7.13; NH 9.81
N115	8.76	(8.93)	115.5	4.92	49.5	2.89	
T116	7.59	(7.59)	119.3	3.89	61.3	3.88	$C\gamma H_3$ 1.17
D117	8.53	(8.54)	126.9	4.40	51.6	2.72, 2.67	
A118	8.84	(8.94)	133.3	3.80	51.5	1.19	
A119	8.69	(8.71)	120.4	3.90	50.8	1.43	
S120	7.64	(7.67)	113.8	4.27	57.0	3.98	
L121	7.66	(7.65)	123.3	4.39	49.7	1.74	
I122	6.91	(6.91)	120.6	3.49	61.1	1.73	
G123	8.78	(8.77)	116.4	4.35, 3.85	41.3		
E124	8.13	(8.14)	120.8	4.57	51.5	2.16	
E125	8.99	(9.07)	121.0	5.22	51.5	2.19, 2.03	
L126	8.71	(8.73)	122.6	5.47	48.4	1.55	
Q127	9.16	(9.18)	122.1	5.27	50.8	2.01, 1.66	
V128	8.94	(8.95)	128.8	5.00	57.2	1.97	$C\gamma H_3$ 0.94, 0.84

Table 1 (Continued)

	H^N						
	pH 7.3	pH 5.3	^{15}N	H^α	$^{13}C^\alpha$	H^β	other
D129	9.02	(9.03)	127.4	5.07	48.2	2.83, 2.39	
F130	8.75	(8.76)	121.1	4.96	55.0	3.39	CδH 7.41
L131	8.27	(8.25)	125.3	4.26	52.0	1.54	
D132	7.83	(7.80)	127.9	4.35	52.0	2.65, 2.57	

[a] Values are for the sample in 10 mM sodium phosphate, pH 7.3, and 0.1 mM DTT, at 25 °C, except for assignments in parentheses which are for the sample in 25 mM sodium acetate-d_3, pH 5.3, and 0.1 mM DTT, at 25 °C. Reference standards were as follows: ^1H, H_2O = 4.76 ppm; ^{15}N, external 2.9 M $^{15}NH_4Cl$ in 1 M HCl = 24.9 ppm; ^{13}C, external dioxane = 67.8 ppm.

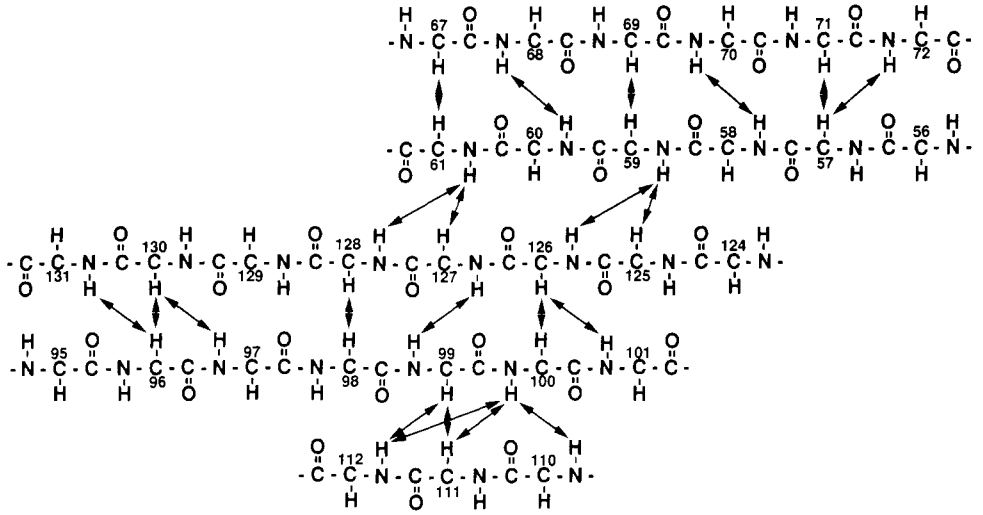

FIGURE 5: Diagram of the β-sheet topology of Raf_{55-132}. Only long-range NOEs between β-strands are shown, depicted as double-headed arrows.

of $^{13}C^\alpha$ to H^β resonances in the 2D ^1H–^{13}C HCCH-TOCSY spectrum.

Sequential assignments were made by following through-bond $^{15}N_{i+1}$–H^N_{i+1}–$^{13}C^\alpha_i$ connectivities in the 3D HN(CO)-CA spectrum (Figure 3). In most cases, these assignments were supported by sequential H^α_i–H^N_{i+1}, H^N_i–H^N_{i+1}, and H^β_i–H^N_{i+1} NOEs in the 2D NOESY and 3D ^1H–^1H–^{15}N NOESY-HSQC spectra (Figure 4).

Sequence-specific assignments were made for 74 of the 76 non-proline residues (Table 1). The chemical shifts of the $^{13}C^\alpha$, ^{15}N, and carbon-bound ^1H resonances were not significantly different between pH 5.3 and 7.3. However, several of the H^N resonances did show significantly different chemical shifts between the two pH values, as indicated in Table 1. Also, for eight of the residues, H^N protons were not strongly observed in heteronuclear experiments at pH 7.3, presumably due to exchange with solvent. For these residues, ^{15}N chemical shifts are reported at pH 5.3 (Table 1).

Secondary Structure and Topology. Assigned NOEs involving H^N protons and H^α–H^α NOEs were measured and classified as small, medium, or large. Elements of secondary structure were identified by first searching for contiguous stretches of large H^α_i–H^N_{i+1} or medium H^N_i–H^N_{i+1} NOEs, which are suggestive of β-strand and α-helical structure, respectively (Wüthrich, 1986). The α-helical regions were verified by the observation of long-range H^α_i–H^N_{i+3} and H^α_i–H^β_{i+3} NOEs (Figure 4) which are characteristic of α-helices (Wüthrich, 1986). The β-strands were verified by the observation of long-range NOEs to other β-strand segments in patterns typical of β-sheets (Wüthrich, 1986) (Figure 5). Regions of secondary structure were further supported by the H^α and $^{13}C^\alpha$ chemical shifts, which were found to be shifted upfield or downfield of standard values in contiguous stretches, indicative of α-helical or β-sheet structure, respectively (Spera & Bax, 1991; Wishart et al., 1992).

A self-consistent β-sheet topology was obtained by analysis of the observed long-range H^α–H^α, H^N–H^α, and H^N–H^N NOEs between β-strands (Figure 5). The β-sheet consists of five strands organized into three antiparallel pairs and one parallel pair (Figures 5 and 6A). Residues 96–130 form a "Greek key" motif, which is a commonly found arrangement of antiparallel β-strands (Richardson, 1977). The N-terminal and C-terminal regions of the protein come together and form a parallel pair in the interior of the β-sheet. There is a 10-residue α-helix in the protein, comprised of residues 79–89. Residues 119–122 may be configured into a second, small helical region. Determination of the detailed tertiary structure of Raf_{55-132} is in progress.

The overall topology of Raf_{55-132} is comparable to that of the protein ubiquitin (Figure 6B), whose structure has been solved by X-ray (Vijay-Kumar et al., 1987) and NMR (Weber et al., 1987; DiStefano & Wand, 1987) methods. This structural similarity was unexpected, since these two proteins exhibit low sequence homology. An attempt was made to align the sequences of Raf_{55-132} and ubiquitin (Figure 6C) using the topology as a guide. Fine adjustment, and alignment of the regions between secondary structure elements, was accomplished by calculating deviations of the H^α chemical shifts from standard values (Wishart et al., 1992) for each protein and attempting to maximize their agreement. Identical residues occur at only eight positions in the optimal alignment, and these are scattered throughout the lenghts of the molecules. The ubiquitin sequence is highly conserved, and the low sequence homology to Raf_{55-132} shows that the purpose of sequence conservation in ubiquitin is not simply to achieve the correct fold. The alignment required the introduction of

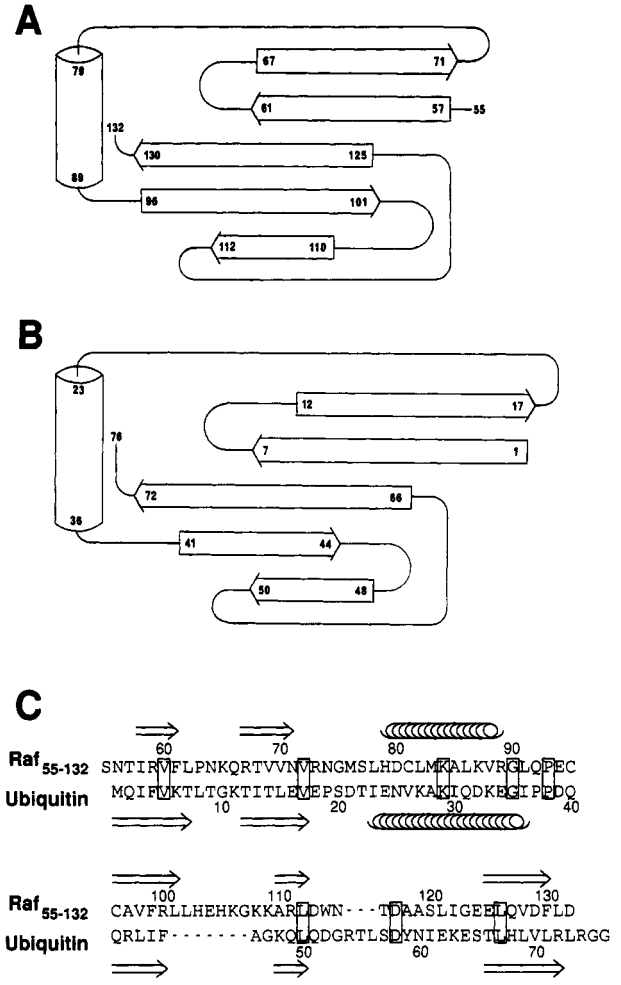

FIGURE 6: Diagram of the overall topologies of (A) Raf_{55-132} and (B) ubiquitin and (C) sequence alignment of the two proteins. β-strands are depicted as arrows, and α-helices are depicted as cylinders. The connecting loop regions are not drawn to scale. The arrangement of the secondary structure elements is not meant to imply a detailed tertiary relationship. In panel C, the sequences of Raf_{55-132} and human ubiquitin were aligned on the basis of topology and comparison of H^{α} chemical shifts, as described in the text. Sequence identities are boxed. The ubiquitin structure corresponds to previously reported work (DeStefano & Wand, 1987).

gaps, indicating that each protein appears to possess a loop that is not present in the other protein—residues 101–107 in Raf_{55-132} and residues 54–56 in ubiquitin. Ubiquitin is known to possess a high thermal stability (Lenkinsiki et al., 1977). This suggests that the structure observed for Raf_{55-132} represents an intrinsically stable domain and further suggests that this structure is adopted by residues 55–132 within the intact Raf-1 protein.

Raf_{55-132} appears to represent a small, self-contained domain that mediates binding to another protein. Ubiquitin has no detectable Ras-binding activity in our assay system (Scheffler et al., 1994). However, the structural similarity suggests that ubiquitin, or other proteins with a similar fold, might be capable of participating in other transient protein-protein interactions. There are at least four proteins with substantial (>20%) sequence homology to ubiquitin (Jentsch et al., 1991), which presumably have a ubiquitin-like fold: (1) v-ubi, a protein from baculovirus (Guarino, 1990); (2) Gdx, encoded by a gene on the human X chromosome (Toniolo et al., 1988); (3) BAT-3, encoded by a gene from the human major histocompatibility complex class III region (Banerji et al., 1990); and (4) UCRP, a protein induced by β-interferon treatment (Knight et al., 1988). Thus far, no specific function has been ascribed to any of these proteins. The established role of ubiquitin, covalent attachment to proteins as a tag for degradation (Hershko & Ciechanover, 1982), has not provided a good model for the action of these ubiquitin-like proteins. Their structural homology to Raf-1 may suggest alternate potential functions.

It is also intriguing that ubiquitin is initially translated with a C-terminal extension of 52–80 residues and that this extension contains a sequence pattern which is proposed to form a zinc finger (Redman & Rechsteiner, 1989). In Raf-1, the 55–132 region is followed by a putative zinc finger domain, residues 151–168 (Warne et al., 1993). One of the extended ubiquitin protein hybrids, ubiquitin-S27a, has been reported to be an early growth response protein and is found at elevated levels in human colorectal carcinoma cells (Wong et al., 1993). This provides two cases in which a ubiquitin-fold/zinc-finger structural motif is linked to transmission of cell growth signals.

ACKNOWLEDGMENT

We gratefully acknowledge the DNA sequencing support of D. Larigan and J. Levine. We thank V. Madison for a critical reading of the manuscript, and J. Birktoft for helpful discussions.

REFERENCES

Banerji, J., Sands, J., Strominger, J. L., & Spies, T. (1990) *Proc. Natl. Acad. Sci. U.S.A. 87*, 2374–2378.
Barbacid, M. (1987) *Annu. Rev. Biochem. 56*, 779–827.
Bax, A., Clore, G. M., & Gronenborn, A. M. (1990) *J. Magn. Reson. 88*, 425–431.
Bodenhausen, G., & Ruben, D. J. (1980) *Chem. Phys. Lett. 69*, 185–188.
Bonner, T. I., Oppermann, H., Seeburg, P., Kerby, S. B., Gunnell, M. A., Young, A. C., & Rapp, U. R. (1986) *Nucleic Acids. Res. 14*, 1009–1015.
Bruschweiler, L., & Ernst, R. R. (1983) *J. Magn. Reson. 53*, 521–528.
Chung, C. T., Niemela, S. L., & Miller, R. H., (1989) *Proc. Natl. Acad. Sci. U.S.A. 86*, 2172–2175.
Davis, A. L., Keeler, J., Laue, E. D., & Moskau, D. (1992) *J. Magn. Reson. 98*, 207–216.
DiStefano, D. L., & Wand, A. J. (1987) *Biochemistry 26*, 7272–7281.
Farmer, B. T., II, Venters, R. A., Spicer, L. D., Wittekind, M. G., & Muller, L. (1992) *J. Biomol. NMR 2*, 195–202.
Gibbs, J. B., Schaber, M. D., Allard, W. J., Sigal, I. S., & Scolnick, E. M. (1988) *Proc. Natl. Acad. Sci. U.S.A. 85*, 5026–5030.
Griesinger, C., Otting, G., Wüthrich, K., & Ernst, R. R. (1988) *J. Am. Chem. Soc. 110*, 7870–7872.
Guarino, L. (1990) *Proc. Natl. Acad. Sci. U.S.A. 87*, 409–413.
Heidecker, G., Kolch, N., Morrison, D. K., & Rapp, U. R. (1992) *Adv. Cancer Res. 58*, 53–73.
Hershko, A., & Ciechanover, A. (1982) *Annu. Rev. Biochem. 51*, 335–364.
Jentsch, S., Seufert, W., & Hauser, H.-P. (1991) *Biochim. Biophys. Acta 1089*, 127–139.
Kay, L. E., Ikura, M., Tschudin, R., & Bax, A. (1990) *J. Magn. Reson. 89*, 496–514.
Knight, E., Fahey, D., Cordova, B., Hillman, M., Kutny, R., Reich, N., & Blomstrom, D. (1988) *J. Biol. Chem. 263*, 4520–4522.
Lenkinsiki, R. E., Chen, D. M., Glickson, J. D., & Goldstein, G. (1977) *Biochim. Biophys. Acta 94*, 126–130.
Macura, S., & Ernst, R. R. (1980) *Mol. Phys. 41*, 95–117.
Marion, D., Ikura, M., Tschudin, R., & Bax, A. (1989) *J. Magn. Reson. 85*, 393–399.
McCoy, M. A., & Mueller, L. (1992) *J. Am. Chem. Soc. 114*, 2108–2112.

Moodie, S. A., Willumsen, B. M., Weber, M. J., & Wolfman, A. (1993) *Science 260*, 1658–1661.
Morrison, D. K. (1990) *Cancer Cells 2*, 377–381.
Mueller, L. (1979) *J. Am. Chem. Soc. 101*, 4481–4484.
Nagayama, K. (1986) *J. Magn. Reson. 66*, 240–249.
Patt, S. L. (1992) *J. Magn. Reson. 96*, 94–102.
Piantini, U., Sorenson, O. W., & Ernst, R. R. (1982) *J. Am. Chem. Soc. 104*, 6800–6801.
Redman, K. L., & Rechsteiner, M. (1989) *Nature 338*, 438–440.
Richardson, J. (1977) *Nature 268*, 495–500.
Rubinfeld, B., Wong, G., Bekesi, E., Wood, A., Heimer, E., McCormick, F., & Polakis, P. (1991) *Int. J. Pept. Protein Res. 38*, 47–53.
Sambrook, J., Fritsch, E. F., & Maniatis, T. (1989) *Molecular Cloning: A Laboratory Manual*, 2nd ed., Cold Spring Harbor Laboratory, Cold Spring Harbor, NY.
Scheffler, J. E., Waugh, D. S., Bekesi, E., Kiefer, S. E., Losardo, J. E., Neri, A., Prinzo, K. M., Tsao, K.-L., Wegrzynski, B., Emerson, S. D., & Fry, D. C. (1994) *J. Biol. Chem.* (in press).
Shaka, A. J., Lee, C. J., & Pines, A. (1988) *J. Magn. Reson. 77*, 274–293.
Spera, S., & Bax, A. (1991) *J. Am. Chem. Soc. 113*, 5490–5492.
Studier, F. W., Rosenberg, A. H., Dunn, J. J., & Dubendorff, J. W. (1991) *Methods Enzymol. 185*, 60–89.
Toniolo, D., Perisco, M. & Alcalay, M. (1988) *Proc. Natl. Acad. Sci. U.S.A. 85*, 851–855.
Van Aelst, L., Barr, M., Marcus, S., Polverino, A., & Wigler, M. (1993) *Proc. Natl. Acad. Sci. U.S.A. 90*, 6213–6217.
Vijay-Kumar, S., Bugg, C. E., & Cook, W. J. (1987) *J. Mol. Biol. 194*, 531–544.
Vojtek, A. B., Hollenberg, S. M., & Cooper, J. A. (1993) *Cell 74*, 205–214.
Warne, P. H., Viciana, P. R., & Downward, J. (1993) *Nature 364*, 352–355.
Weber, P. L., Brown, S. C., & Mueller, L. (1987) *Biochemistry 26*, 7282–7290.
Williams, N. G., Paradis, H., Agarwal, S., Charest, D. L., Pelech, S. L., & Roberts, T. M. (1993) *Proc. Natl. Acad. Sci. U.S.A. 90*, 5772–5776.
Wishart, D. S., Sykes, B. D., & Richards, F. M. (1992) *Biochemistry 31*, 1647–1651.
Wong, J. M., Mafune, K., Yow, H., Rivers, E. N., Ravikumar, T. S., Steele, G. D., & Chen, L. B. (1993) *Cancer Res. 53*, 1916–1920.
Wüthrich, K. (1986) *NMR of Proteins and Nucleic Acids*, John Wiley, New York.
Zhang, X., Settleman, J., Kyriakis, J. M., Takeuchi-Suzuki, E., Elledge, S. J., Marshall, M. S., Bruder, J. T., Rapp, U. R., & Avruch, J. (1993) *Nature 364*, 308–313.